JACS
JOURNAL OF THE AMERICAN CHEMICAL SOCIETY
pubs.acs.org/JACS
Article

Unprecedented Small Molecule-Based Uniform Two-Dimensional Platelets with Tailorable Shapes and Sizes

Yanjun Gong,[‖] Chuanqin Cheng,[‖] Hongwei Ji, Yanke Che,* Ling Zang, Jincai Zhao, and Yifan Zhang*

Cite This: *J. Am. Chem. Soc.* 2022, 144, 15403−15410
Read Online
ACCESS | Metrics & More | Article Recommendations | Supporting Information

ABSTRACT: Fabrication of uniform two-dimensional (2D) structures from small molecules remains a formidable challenge for living self-assembly despite its great success in producing uniform one-dimensional (1D) structures. Here, we report the construction of unprecedented uniform 2D platelets with tailorable shapes and controlled sizes by creating new nuclei from a donor−acceptor (D−A) molecule and 1-hexanol to initiate 2D living self-assembly. We demonstrate that the D−A molecule undergoes 1-hexanol-induced twisting to form continuous alternative hydrogen bonds in-between under electrostatic attraction, which in turn forms a new nucleus. This connection architecture of the new nucleus allows to simultaneously regulate the growth rate of **1** in two dimensions to generate 2D platelets of distinct shapes through simply varying the amount of 1-hexanol relative to hexane. Furthermore, the living nature of the new nucleus enables seeded growth of complex concentric multiblock 2D heteroplatelets by sequential and alternative addition of different D−A molecules. Interestingly, the resulting 2D platelets obtained by such living self-assembly exhibit enhanced photostability compared to those obtained by conventional self-assembly without the involvement of 1-hexanol.

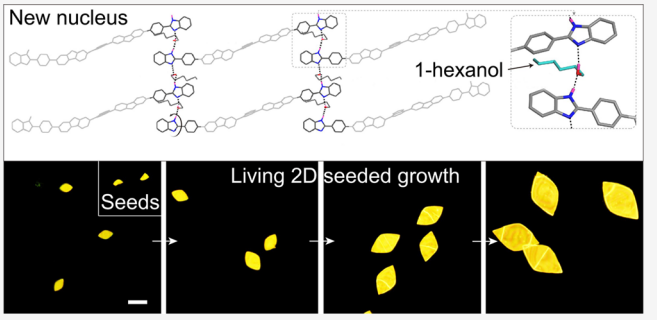

INTRODUCTION

Two-dimensional (2D) materials have attracted extensive attention because of their unique structure-related potential in electronics, biomedicine, catalysis, and sensing and as membranes for separation and filtration.[1−7] Among various methods for rational design and synthesis of 2D organic materials, living seeded self-assembly has emerged as a powerful strategy for fabricating uniform 2D polymers with controlled shapes and sizes. Prominent examples are the block copolymer-based systems pioneered by Manners and coworkers, which have been successfully fabricated into uniform and complex 2D structures via crystallization-driven living self-assembly.[8−11] However, compared with polymers, living self-assembly of small molecules into uniform 2D structures with tailorable shapes and sizes remains a formidable challenge. To date, only irregular 2D structures, rather than well-defined uniform morphologies, can be achieved with specific porphyrin molecules,[12,13] which is far from the precise control over sizes and shapes as attained for 2D polymers.[8−11]

In recent years, two groundbreaking methods, that is, kinetically trapping the monomer in a metastable aggregate[14] or in an inactive molecular state (e.g., via intramolecular hydrogen bonding)[15] have been developed to restrict the fast nucleation process. This thus allows access to living self-assembly of small molecules into 1D structures with precisely controlled lengths.[14−26] However, despite the aforementioned many advances, these methods have not yet provided a promising route for the fabrication of uniform 2D structures from small molecules. The formation of uniform 2D structures from small molecules generally requires relatively weak intermolecular interactions in one dimension but synchronously controllable interactions in the other two dimensions. These requirements may augment the molecular complexity, conflicting with the molecular structural requirements in the methods for living self-assembly of 1D structures. Thus, a groundbreaking way to achieve living 2D self-assembly of small molecules needs to be developed but remains unexplored.

In this work, we report the construction of unprecedented uniform 2D platelets with tailorable shapes and sizes from a donor−acceptor (D−A) molecule, **1** (Figure 1a) via a unique living 2D self-assembly strategy. Unlike the restriction of fast nucleation by kinetically trapping the monomer in metastable aggregates[14] or in an inactive molecular state,[15] the slow generation of new nuclei is the key to achieving living 2D seeded growth of **1** in solution and *in situ* on the surface. Crystallographic analysis demonstrates that **1** undergoes

Received: July 15, 2022
Published: August 11, 2022

https://doi.org/10.1021/jacs.2c07480
J. Am. Chem. Soc. 2022, 144, 15403−15410

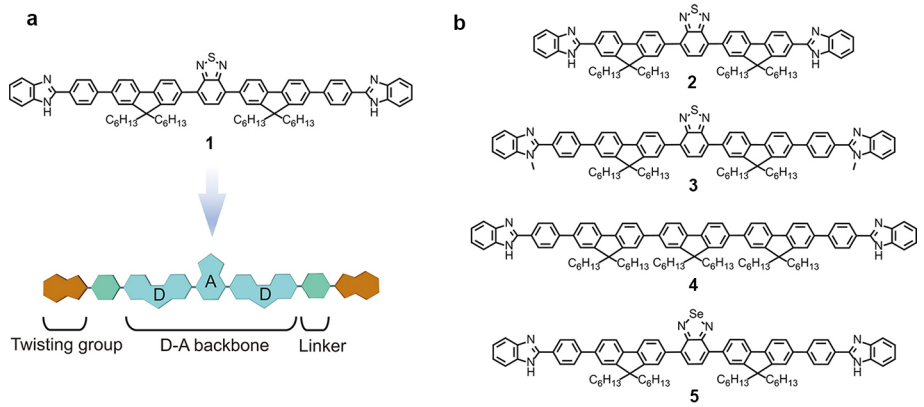

Figure 1. (a) Molecular structure and schematic presentation of **1**. (b) Molecular structures of **2**−**5**.

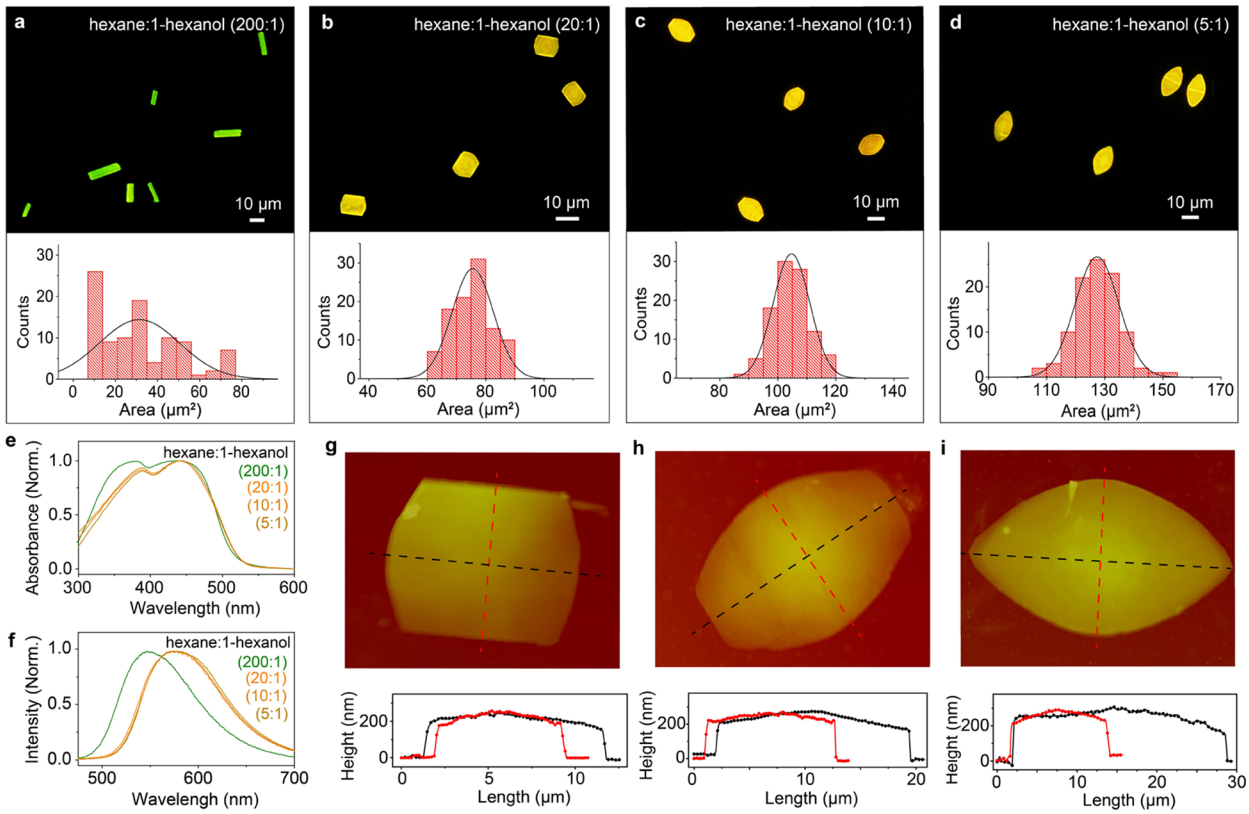

Figure 2. (a−d) Fluorescence-mode optical images and statistical histogram of the area dispersities of green-emissive crystals and yellow-emissive 2D platelets from **1** at a volume ratio of hexane to 1-hexanol of 200:1, A_w = 42.9 μm^2, A_n = 32.3 μm^2, A_w/A_n = 1.32 (a); 20:1, A_w = 67.1 μm^2, A_n = 66.2 μm^2, A_w/A_n = 1.02 (b); 10:1, A_w = 117.5 μm^2, A_n = 116.5 μm^2, A_w/A_n = 1.01 (c); and 5:1, A_w = 135.6 μm^2, A_n = 132.4 μm^2, A_w/A_n = 1.02 (d). UV−vis absorption (e) and fluorescence spectra (f) of 2D platelets formed in various 1-hexanol/hexane mixtures. (g−i) AFM height images and corresponding height profiles of rectangular- (g), hexagonal- (h), and diamond-like (i) yellow-emissive 2D platelets.

twisting to form continuous alternative hydrogen bonds with 1-hexanol under electrostatic attraction, which in turn slowly forms a new nucleus. This connection architecture allows the simultaneous control of the growth of **1** in two dimensions.

Specifically, simply varying the volume ratios of hexane to 1-hexanol enables regulation of the growth rate of 2D platelets in different directions, thus generating yellow-emissive 2D platelets with distinct shapes. Furthermore, upon sequential and alternative addition of different D−A molecules (i.e., **1** and **5**, Figure 1), the living seeded 2D self-assembly enables the formation of complex concentric multiblock heteroplatelets of different shapes. In sharp contrast, without the involvement of 1-hexanol, **1** undergoes conventional self-assembly, forming high-dispersity green-emissive crystals, which exhibit typical "nonliving" self-assembly behavior. Intriguingly, the yellow-emissive 2D platelets obtained via living seeded self-assembly exhibit enhanced photostability compared to the green-emissive crystals obtained via conventional self-assembly in the absence of 1-hexanol. The new living self-assembly strategy reported herein, along with the novel molecular design and engineering, provides an unprecedented route to fabricate uniform 2D structures with tailorable sizes and shapes that may find broad applications in organic electronics, photocatalysis, and chemical/biological sensing.

https://doi.org/10.1021/jacs.2c07480
J. Am. Chem. Soc. 2022, 144, 15403−15410

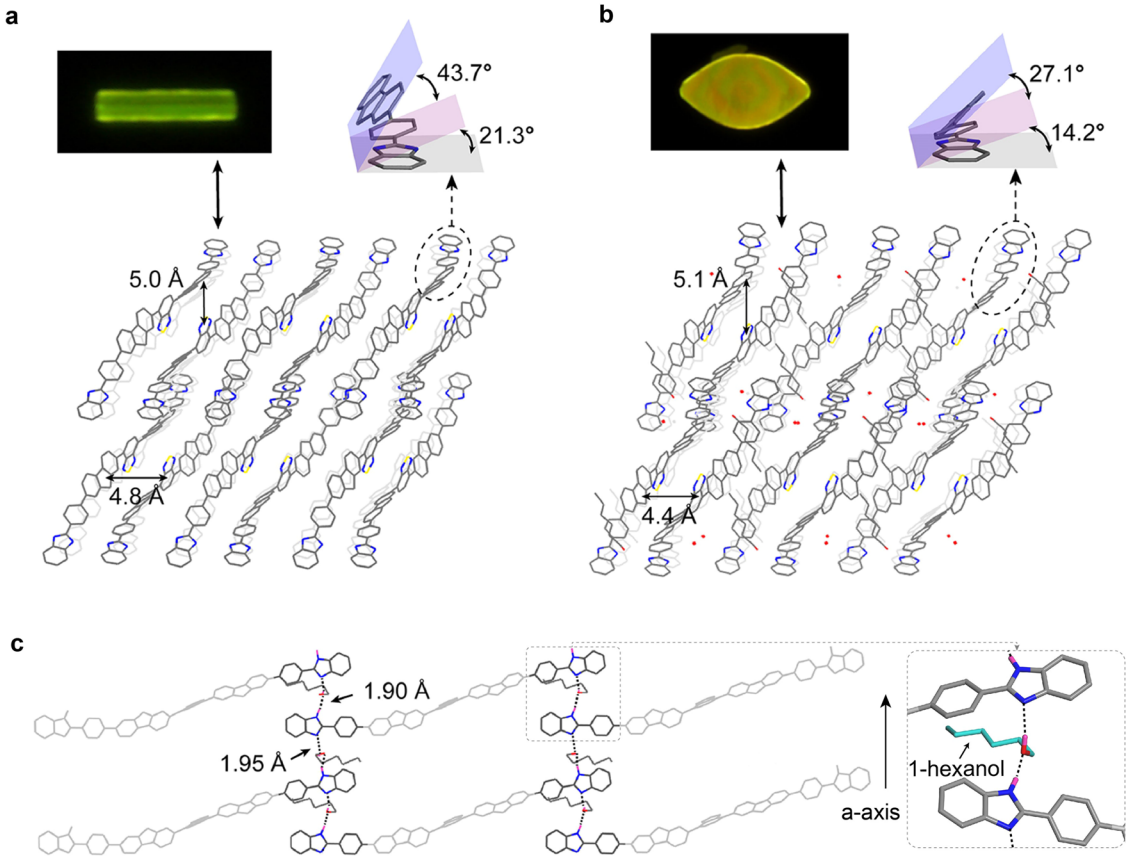

Figure 3. (a, b) Fluorescence-mode optical images and corresponding single-crystal structures of a green-emissive lath-like crystal (a) and a yellow-emissive platelet (b). (c) Continuous alternative intermolecular hydrogen bonds between 1-hexanol and **1** along the *a*-axis in a yellow-emissive 2D platelet.

RESULTS AND DISCUSSION

Molecular Design. Molecule **1** designed in the present study has three key parts: the D−A backbone comprising fluorene (D) and benzothiadiazole (A) units, the phenyl group as a linker, and the benzimidazole group as a twisting group (Figure 1a). The D−A backbone is expected to endow the relatively strong electrostatic attraction between **1**. The benzimidazole group that is connected to the D−A backbone through the phenyl unit is expected to afford flipper-like twisting upon external intervention (e.g., via hydrogen bonding) because of the linker-alleviated bulky repulsion. To highlight the crucial roles of the three parts in **1**, we synthesized control molecules **2**−**5** (Figure 1b) and compared their self-assembly behaviors. Molecule **2** has the same D−A backbone and benzimidazole group but lacks the phenyl group to reduce steric repulsion. Molecule **3** has all three parts but with the benzimidazole group methylated to prevent it from being capable of forming hydrogen bonds. Molecule **4** has the phenyl linker and benzimidazole group but lacks the D−A backbone for strong intermolecular electrostatic interactions. Molecule **5** has a molecular structure similar to **1** but replacing the benzothiadiazole group with the benzoselenadiazole group, which is expected to undergo similar self-assembly behaviors as **1**. The detailed synthesis procedures and characterizations of molecules **1**−**5** are provided in the Supporting Information.

Formation of Different 2D Platelets. Self-assembly of **1** was performed by adding different volumes of hexane (poor solvent) into a 1-hexanol solution (good solvent) of **1** (0.5 mg/mL, 0.1 mL), followed by aging the resulting hexane/1-hexanol mixtures for 24 h (the volume ratios of hexane to 1-hexanol ranged from 200:1 to 5:1). Interestingly, two types of crystalline assemblies, that is, green-emissive crystals and yellow-emissive platelets, were formed in various hexane/1-hexanol mixtures. As revealed by fluorescence-mode optical microscopy (Figures 2a−d and S1), green-emissive lath-like crystals were formed from **1** for a volume ratio of hexane to 1-hexanol greater than 100:1, while yellow-emissive platelets with different shapes (rectangular, hexagonal, and diamond) were fabricated from **1** for volume ratios of hexane to 1-hexanol less than 30:1. Moreover, a mixture of green-emissive crystals and yellow-emissive platelets was fabricated for volume ratios of hexane to 1-hexanol between 100:1 and 30:1 (Figure S2). Unexpectedly, the yellow-emissive 2D platelets with the three shapes have a narrow area dispersity ($A_w/A_n \leq 1.02$; see Figures 2b−d), which is in sharp contrast to the green-emissive lath-like crystals with a wide area dispersity ($A_w/A_n = 1.32$; see Figure 2a). These observations suggest that **1** can adopt different molecular packing, depending on the volume ratios of hexane/1-hexanol in the solvent mixture. Optical characterization demonstrated that the yellow-emissive 2D platelets have the same absorption (Figure 2e) and fluorescence spectra (Figure 2f) despite the distinct shapes but exhibit a remarkable 38 nm redshift in the fluorescence emission compared to the green-emissive crystals (Figure 2f).

Given the solvent circumstance, more 1-hexanol may be involved in the yellow-emissive 2D platelets than the green-emissive crystals, which have a negligible effect on the absorption but can interact with the excited D−A molecule

https://doi.org/10.1021/jacs.2c07480
J. Am. Chem. Soc. 2022, 144, 15403−15410

1 to induce the prominent red-shifted emission, being typical characteristics of D−A molecules. These results indicate that the same molecular packing is shared among the yellow-emissive platelets with the three different shapes, but the packing is distinct from that of the green-emissive crystals. This conclusion is further supported by experimental results from powder X-ray diffraction (XRD) and selected area electron diffraction (SAED). The XRD results show the same lamellar structure for the yellow-emissive platelets of the three shapes along the thickness direction, with an interlayer height of 1.6 nm (Figure S3). In contrast, the green-emissive lath-like crystals exhibit a distinct XRD pattern with a d-spacing of 1.3 nm in the thickness direction (Figure S4). The SAED patterns of the yellow-emissive 2D platelets with the different shapes demonstrate the same intraplanar molecular orientation of **1** (Figure S5). Of note, atomic force microscopy (AFM) revealed that the yellow-emissive 2D platelets have a uniform thickness of 210 nm regardless of the different shapes and areas (Figure 2g−i). The smooth and flat surface of these yellow-emissive 2D platelets was further confirmed by scanning electron microscopy (SEM) (Figure S6).

Creation of New Nuclei To Initiate Living Self-Assembly. Given that 1-hexanol forms hydrogen-bonded clusters itself when the volume ratio of hexane to 1-hexanol is greater than 100:1,[27] we hypothesized that 1-hexanol was not involved in the molecular packing within the green-emissive crystals. However, 1-hexanol might affect the formation of the yellow-emissive 2D platelets via hydrogen bonding with **1** when the volume ratio of hexane to 1-hexanol is greatly decreased. Green-emissive crystals with the same XRD pattern (Figure S4) were fabricated by using tetrahydrofuran instead of 1-hexanol as the good solvent, supporting the hypothesis that 1-hexanol was not involved in the formation of green-emissive lath-like crystals. To gain precise information on the molecular packing of **1** and insight into the role of 1-hexanol in the formation of yellow-emissive 2D platelets, single-crystal X-ray diffraction (SCXRD) analysis of green and yellow single crystals was performed. As shown in Figure 3a, molecule **1** adopts a twisted backbone structure within the green-emissive crystal, which leads to intermolecular distances of 4.8 and 5.0 Å along the *a*-axis and *c*-axis, respectively, while the long bulky alkyl groups in **1** further increase the intermolecular distance to 17.0 Å along the *b*-axis. The relatively large intermolecular distances between neighboring **1** are apparently beyond π-interactions but are attributed to typical electrostatic attractions of D−A molecules. Therefore, electrostatic attractions mainly give rise to the formation of green-emissive lath-like crystals. Moreover, the larger electrostatic attraction along the *a*-axis, as reflected by the shorter intermolecular distance (4.8 Å), yields platelets with an elongated shape along the *a*-axis. For the yellow-emissive 2D platelets, as expected, 1-hexanol was involved in the formation of the crystalline structure (Figure 3b, c). Moreover, 1-hexanol acts as both a hydrogen-bond donor and acceptor for two neighboring benzimidazole groups, and thus continuously connects molecules **1** along the *a*-axis via hydrogen bonding (Figure 3b,c). Remarkably, the benzimidazole group and the phenyl linker adopt certain flipper-like twisting to accommodate the hydrogen bonding with 1-hexanol, and the benzimidazole-phenyl backbone becomes more coplanar compared to the case of green-emissive crystals. The structural changes should provide a route to the slow formation of a new nucleus, which in turn simultaneously control over the growth of **1** in two dimensions to form yellow-emissive 2D platelets. Additional solid evidence comes from the fact that green-emissive lath-like crystals pregrown in a hexane/1-hexanol mixture at a volume ratio of 200:1 slowly transformed into yellow-emissive crystals after 5 days of immersion in a hexane/1-hexanol mixture with a volume ratio of 5:1. The slow diffusion of 1-hexanol into the green-emissive crystals induced twisting of **1** to form the hydrogen bonding, transforming them into yellow-emissive crystals (Figure S7). Given the cocrystal nature (i.e., composed of **1** and 1-hexanol) of the new nucleus, we expected that the volume ratio of hexane to 1-hexanol would effectively affect the growth rate of yellow-emissive 2D platelets. As shown in Figure S8, decreasing the volume ratio of hexane to 1-hexanol from 20:1 to 5:1 greatly retards the growth of 2D platelets from 8 to 36 h, which is attributed to the formation of isolated hydrogen-bonded clusters between **1** and more 1-hexanol molecules with higher probability than the formation of continuous alternative hydrogen bonds between **1** and 1-hexanol. This intervention in the growth rate would also modulate the relative growth rate of **1** along two dimensions, which can well explain the aforementioned formation of yellow-emissive 2D platelets with different shapes.

To highlight the structural rationality of **1** for the fabrication of 2D structures with tailorable shapes, self-assembly of molecules **2**−**5** was performed under identical conditions to explore whether they can form similar 2D structures. Figures S9 and S10 show that similar nanofibers were self-assembled from **2** without the phenyl linker in various hexane/1-hexanol mixtures. Fluorescence spectra (Figure S11) demonstrate that the nanofibers formed in various hexane/1-hexanol mixtures share the same molecular packing, indicating that no different nuclei were formed as with **1**. Because of the increased solubility of **3**, likely from the added methyl group, no aggregates were formed from **3** as tested in the same hexane/1-hexanol mixtures. Bundled nanofibers were formed from **4** via π−π stacking and hydrophobic interactions in various hexane/1-hexanol mixtures (Figures S12 and S13). Likewise, the fluorescence spectra (Figure S14) and XRD patterns (Figure S15) demonstrate that all nanofibers formed from **4** share the same molecular packing. These results suggest that the relatively strong electrostatic attractions of D−A molecules are required to bring molecules close enough for the formation of continuous alternative hydrogen bonds with 1-hexanol. As expected, 2D platelets were also fabricated from **5** under identical conditions (Figure S16), despite the variations in shapes likely as a result of the increased electrostatic attraction in **5**. Of note, the varied acceptor (A) group, the benzoselenadiazole group, in **5** led to the different emission (orange) of the resulting 2D platelets. SCXRD analysis of the orange-emissive 2D platelet from **5** (Figure S17) revealed that **5** and 1-hexanol were connected by the continuous, alternative hydrogen bonding, similar to the aforementioned **1** and 1-hexanol (Figure S17 and Table S1). These observations together point to the indispensability of the three parts in **1** and **5**, that is, the D−A backbone, the phenyl group as a linker, and the benzimidazole group as a twisting group, in combining the second component (1-hexanol) to yield a new nucleus, leading to the formation of shape-defined 2D platelets.

We noticed that the generation of the new nucleus with the involvement of 1-hexanol gave rise to the formation of uniform yellow-emissive 2D platelets with a narrow area dispersity ($A_w/A_n \leq 1.02$; see Figure 2b−d), whereas spontaneous self-assembly of **1** itself yielded green-emissive lath-like crystals

https://doi.org/10.1021/jacs.2c07480
J. Am. Chem. Soc. 2022, 144, 15403−15410

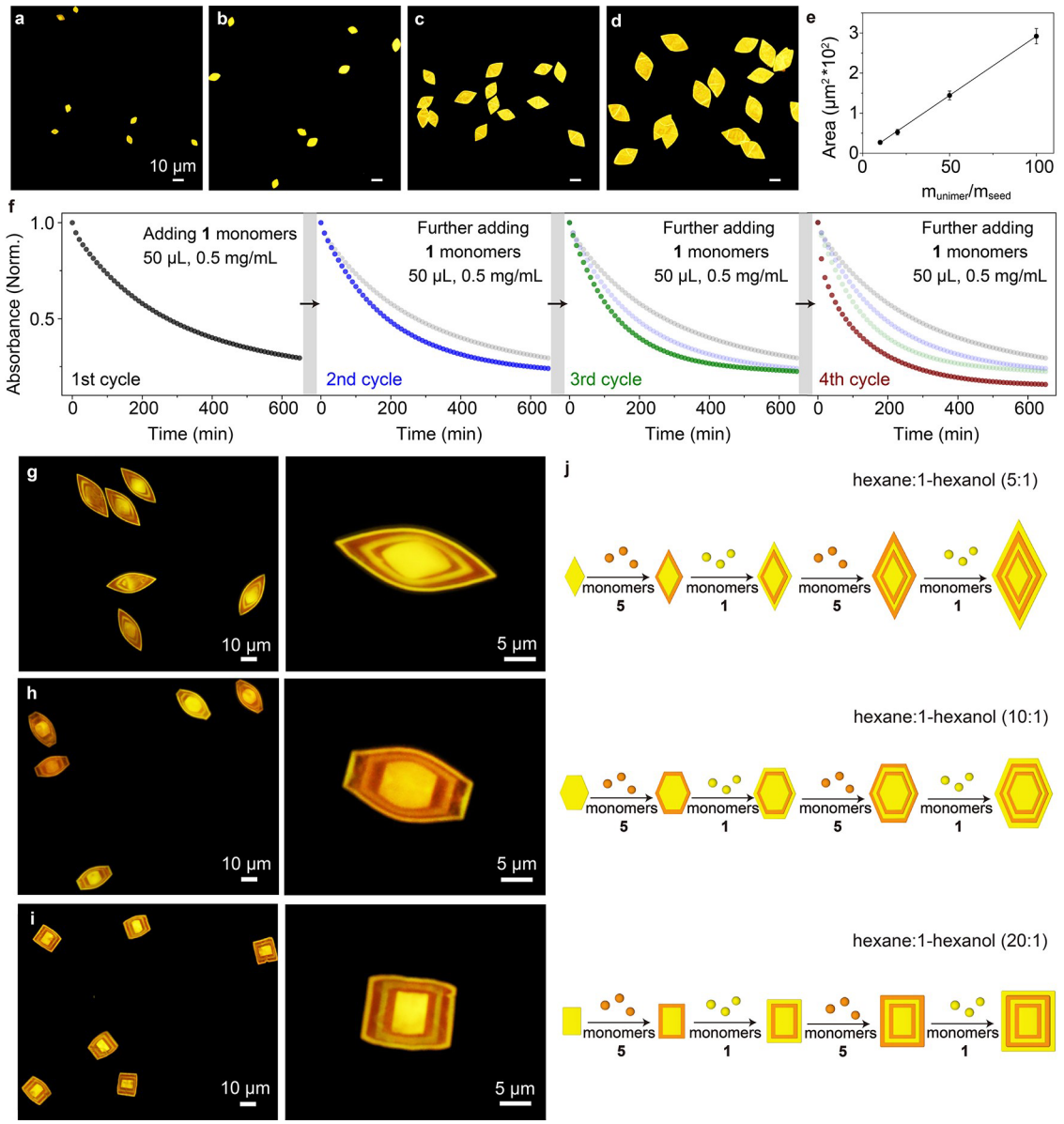

Figure 4. (a–d) Fluorescence-mode optical images of yellow-emissive diamond-like 2D platelets formed upon the addition of a certain volume of **1** (0.1 mg/mL) in a hexane/1-hexanol (v/v, 5:1) mixture to the seed solution (0.1 mL, 0.025 mg/mL), leading to monomer-to-seed mass ratios ($m_{monomer}/m_{seed}$) of 10:1 (a), 20:1 (b), 50:1 (c), and 100:1 (d). (e) Areas of the yellow-emissive diamond-like 2D platelets as a function of the monomer-to-seed mass ratio. (f) Time-dependent absorbance at 345 nm in the four cycles of sequential addition of **1** monomers to seed solution (0.1 mL, 0.025 mg/mL), showing the accelerated rate of the growth of 2D platelets. (g–i) Fluorescence-mode optical images of the uniform diamond- (g), hexagonal- (h), and rectangular-like (i) concentric multiblock 2D heteroplatelets. (j) Schematic diagram illustrating the seeded growth of uniform concentric multiblock 2D heteroplatelets by sequential, alternate addition of **1** and **5** monomers.

with a wide area dispersity (A_w/A_n = 1.32; see Figure 2a). These observations motivated us to investigate the possibility of "living" 2D seeded self-assembly of **1** in hexane/1-hexanol mixtures. Prefabricated yellow-emissive rectangular-like 2D platelets were sonicated for 8 h at −20 °C to produce irregular fragments with areas ranging from 600 nm^2 to 7.2 μm^2 (Figure S18) that served as seeds for the following living 2D seeded growth. The living seeded self-assembly upon addition of a solution of **1** in a hexane/1-hexanol mixture to the seed solution in the same hexane/1-hexanol mixture was investigated by fluorescence optical microscopy. As shown in Figures 4a and S19, after the addition of a certain monomer solution, uniform yellow-emissive 2D platelets with increased size quickly formed in 2 h, and no formation of new nuclei (i.e., small-size 2D platelets) was observed. Addition of **1** monomers with higher monomer-to-seed mass ratios into the corresponding hexane/1-hexanol mixture led to uniform 2D platelets with increased areas while retaining the original shape (Figure 4b–d). Quantitative experiments demonstrated that the areas of the resulting yellow-emissive 2D platelets exhibited a linear dependence on the monomer-to-seed mass ratios (Figures 4e and S19), which suggest a living seeded self-assembly.[10,14]

Further support for the living growth of 2D platelets came from experiments where the same amount of **1** monomers was sequentially further added to the seed solution in the same hexane/1-hexanol mixture. Figures 4f, S20, and S21 show the kinetic absorbance changes and morphological growth in the

https://doi.org/10.1021/jacs.2c07480
J. Am. Chem. Soc. 2022, 144, 15403−15410

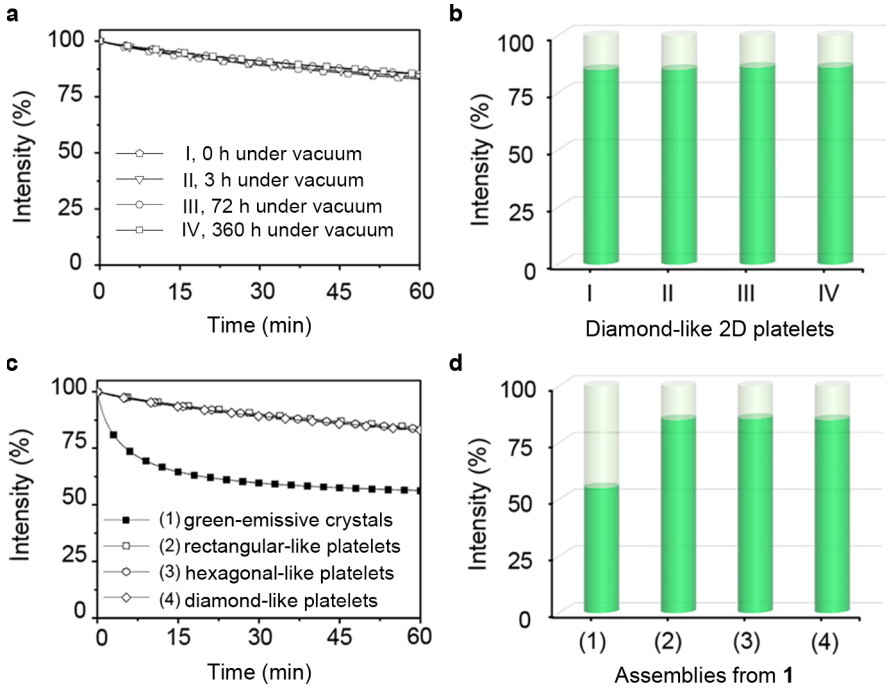

Figure 5. (a) Fluorescence intensity of yellow-emissive diamond-like 2D platelets placed under vacuum for four different durations at 60 °C (I, II, III, and IV) as a function of UV irradiation time (385 nm, 0.053 mW/cm^2). The fluorescence intensity was monitored in the range of 550 to 600 nm. (b) Fluorescence intensity of the four diamond-like 2D platelets after 1 h of UV irradiation. (c) Fluorescence intensity of four different assemblies from **1** as a function of UV irradiation time (385 nm, 0.053 mW/cm^2), which was monitored in the range of 520 to 570 nm for (**1**) and 550 to 600 nm for (**2**–**4**). (d) Fluorescence intensity of the four assemblies from **1** after 1 h of UV irradiation.

four cycles of the sequential addition of **1** monomers (50 μL, 0.5 mg/mL) to the seed solution (0.1 mL, 0.025 mg/mL). Again, a linear relationship between the statistical areas of the resulting yellow-emissive 2D platelets and accumulated **1** monomers in cycles was observed (Figure S21), supportive of the living seeded growth of **1**. Notably, an accelerated rate of the seeded self-assembly of **1** with the following cycles was observed (Figure 4f), which is in sharp contrast to the reduced rate in the increasing cycles observed in the living 1D self-assembly.[14] Herein, the increasing living sites with the enlarged circumference of 2D platelets should result in the accelerated rate in 2D living self-assembly. Interestingly, yellow-emissive 2D platelets with different shapes were successfully grown from the same seeds prepared from rectangular platelets by sonication. These results are consistent with the aforementioned mechanism, in which tuning the volume fraction of 1-hexanol relative to hexane enables modulation of the hydrogen-bond interactions and thus of the growth rate of 2D platelets along different directions to define the resulting shape. These phenomena are in contrast to those of polymers, in which polymer seeds possess a morphological memory effect.[10]

To monitor the living 2D seeded growth of **1**, we also developed an in situ surface self-assembly method and used confocal laser scanning microscopy (CLSM) to monitor the 2D seeded growth process in solution. The seeds were first anchored on the bottom surface of a cell culture dish by drop casting 2 μL of highly diluted seed solution (0.025 mg/mL) and subsequently adding different hexane/1-hexanol mixtures of **1** monomers for growth. As shown in Figure S22, the seeds prepared from rectangular-like 2D platelets grew into larger 2D platelets in different shapes depending on the volume ratios of hexane to 1-hexanol in the solvent mixture. A linear relationship between the area of 2D platelets and the growth time (Figure S22) clearly demonstrates the continuous 2D growth of **1** on the seeds. We also noticed that the assembled yellow-emissive 2D platelets remained unaltered after 36 h in solution, indicative of their stability (Figure S23). To further explore the capacity of the living 2D seeded self-assembly for complex 2D architectures, sequential and alternative adding of **1** and **5** monomers to the seed solution was performed. As shown in Figure 4g–j, uniform diamond-, hexagonal-, and rectangular-like concentric multiblock 2D heteroplatelets, which exhibited distinct alternative emissions, were fabricated in different hexane/1-hexanol mixtures. These results not only provide clear visualized evidence for the living nature of the above 2D seeded self-assembly but also show the potential of the living seeded self-assembly for the construction of complex 2D architectures. Finally, seeds prepared from the green-emissive crystals using the same sonication method were also used to study the possibility of living self-assembly. As shown in Figure S24, no seeded growth of green-emissive crystals but instead the formation of new green-emissive lath-like crystals was observed, which suggests the necessity of the formed new nucleus with continuous alternative hydrogen bonds with 1-hexanol. Altogether, the above results allow us to conclude that the slow formation of the new nucleus with a unique connection architecture provides an unprecedented route to living 2D self-assembly for the fabrication of 2D structures with tailorable sizes, shapes, and architectures in a controllable way.

Enhanced Photostability of 2D Platelets Prepared from Living Seeded Growth. Considering that 1-hexanol as one crystal component may escape from the yellow-emissive 2D structure, negatively affecting the chemical stability, we evaluated the photostability of 2D platelets in different shapes, which is an important parameter in practical applications such

https://doi.org/10.1021/jacs.2c07480
J. Am. Chem. Soc. 2022, 144, 15403−15410

as fluorescence sensors and imaging.[28−30] Figure 5a, b shows the fluorescence intensity of the diamond-like 2D platelets placed under vacuum for different durations as a function of the continuous UV irradiation time. Clearly, the fluorescence intensity of all the platelets under test exhibited similar decay profiles under UV irradiation, indicative of the high photostability of yellow-emissive 2D platelets. This observation also suggests that 1-hexanol that connects **1** molecules via hydrogen bonding does not easily escape from the crystalline structure, even under vacuum. Of note, the photostability of yellow-emissive 2D platelets is much better than that of green-emissive crystals, for which the fluorescence intensity decreased by more than 40% under identical conditions (Figure 5c, d). We hypothesized that the nonhydrogen-bonded active hydrogen atom in the benzimidazole group gave rise to severe photobleaching and thus decreased photostability of green-emissive crystals. To support this hypothesis, we also tested, as a comparison, the photostability of the film formed from **3**, in which the active hydrogen was methylated. As expected, the photostability of the film formed from **3** was greatly enhanced, becoming comparable to that of yellow-emissive 2D platelets (Figure S25). These results imply that the formation of 1-hexanol-involved new nuclei concurrently provides a promising way to modulate the chemical properties and stability of 2D platelets.

CONCLUSIONS

In conclusion, we have fabricated unprecedented uniform 2D platelets with tailorable shapes and sizes by creating new nuclei from D−A molecule **1** and 1-hexanol to initiate living 2D self-assembly. Crystallographic analysis demonstrates that **1** undergoes molecular twisting to form continuous alternative hydrogen bonds with 1-hexanol under the assistance of electrostatic attraction, which in turn forms a new nucleus. Interestingly, the continuous alternative hydrogen-bonding interactions between 1-hexanol and **1** can be regulated by changing the volume ratio of the binary solvent of hexane and 1-hexanol, which thus modulates the growth rate of 2D platelets in different directions and defines the distinct shapes. The living 2D self-assembly can be used to construct the uniform concentric multiblock 2D heteroplatelets, showing its capacity of building complex 2D architectures. Importantly, the yellow-emissive 2D platelets formed via living 2D seeded self-assembly exhibit enhanced photostability compared to the crystals formed via conventional self-assembly without involvement of 1-hexanol. Such a strategy, that is, creating a new nucleus with a unique 2D connection architecture to afford living 2D self-assembly may be extended to fabricate more complex 2D architectures with controlled sizes and novel functions that have not yet been achieved.

ASSOCIATED CONTENT

Supporting Information

The Supporting Information is available free of charge at https://pubs.acs.org/doi/10.1021/jacs.2c07480.

Synthesis details for compounds **1**−**5**, experimental details, property characterizations, and additional experimental results (PDF)

Accession Codes

CCDC 2171137−2171138 and 2190266 contain the supplementary crystallographic data for this paper. These data can be obtained free of charge via www.ccdc.cam.ac.uk/data_request/cif, or by emailing data_request@ccdc.cam.ac.uk, or by contacting The Cambridge Crystallographic Data Centre, 12 Union Road, Cambridge CB2 1EZ, UK; fax: +44 1223 336033.

AUTHOR INFORMATION

Corresponding Authors

Yanke Che − *Key Laboratory of Photochemistry, CAS Research/Education Center for Excellence in Molecular Sciences, Institute of Chemistry, Chinese Academy of Sciences, Beijing 100190, China; University of Chinese Academy of Sciences, Beijing 100049, China;* orcid.org/0000-0002-9671-3704; Email: ykche@iccas.ac.cn

Yifan Zhang − *Key Laboratory of Photochemistry, CAS Research/Education Center for Excellence in Molecular Sciences, Institute of Chemistry, Chinese Academy of Sciences, Beijing 100190, China; University of Chinese Academy of Sciences, Beijing 100049, China;* orcid.org/0000-0003-1298-5436; Email: yfzhang@iccas.ac.cn

Authors

Yanjun Gong − *Key Laboratory of Photochemistry, CAS Research/Education Center for Excellence in Molecular Sciences, Institute of Chemistry, Chinese Academy of Sciences, Beijing 100190, China; University of Chinese Academy of Sciences, Beijing 100049, China*

Chuanqin Cheng − *Key Laboratory of Photochemistry, CAS Research/Education Center for Excellence in Molecular Sciences, Institute of Chemistry, Chinese Academy of Sciences, Beijing 100190, China; University of Chinese Academy of Sciences, Beijing 100049, China*

Hongwei Ji − *Key Laboratory of Photochemistry, CAS Research/Education Center for Excellence in Molecular Sciences, Institute of Chemistry, Chinese Academy of Sciences, Beijing 100190, China*

Ling Zang − *Department of Materials Science and Engineering, University of Utah, Salt Lake City, Utah 84112, United States;* orcid.org/0000-0002-4299-0992

Jincai Zhao − *Key Laboratory of Photochemistry, CAS Research/Education Center for Excellence in Molecular Sciences, Institute of Chemistry, Chinese Academy of Sciences, Beijing 100190, China; University of Chinese Academy of Sciences, Beijing 100049, China;* orcid.org/0000-0003-1449-4235

Complete contact information is available at: https://pubs.acs.org/10.1021/jacs.2c07480

Author Contributions

‖Y.G. and C.C. contributed equally to this work.

Notes

The authors declare no competing financial interest.

ACKNOWLEDGMENTS

This work was funded by NSFC (Nos. 21925604), National Key Research and Development Program of China (No. 2019YFA0210401), and the Strategic Priority Research Program of Chinese Academy of Sciences (Grant No. XDB36000000).

REFERENCES

(1) Liu, Q.; Zhang, Q.; Shi, W.; Hu, H.; Zhuang, J.; Wang, X. Self-assembly of polyoxometalate clusters into two-dimensional cluster-phene structures featuring hexagonal pores. *Nat. Chem.* **2022**, *14*, 433−440.

(2) Wang, M.; Huang, M.; Luo, D.; Li, Y.; Choe, M.; Seong, W. K.; Kim, M.; Jin, S.; Wang, M.; Chatterjee, S.; Kwon, Y.; Lee, Z.; Ruoff, R. S. Single-crystal, large-area, fold-free monolayer graphene. *Nature* **2021**, *596*, 519−524.
(3) Juarez-Perez, E. J.; Haro, M. Perovskite solar cells take a step forward. *Science* **2020**, *368*, 1309−1309.
(4) Evans, A. M.; Parent, L. R.; Flanders, N. C.; Bisbey, R. P.; Vitaku, E.; Kirschner, M. S.; Schaller, R. D.; Chen, L. X.; Gianneschi, N. C.; Dichtel, W. R. Seeded growth of single-crystal two-dimensional covalent organic frameworks. *Science* **2018**, *361*, 52−57.
(5) Cheng, C.; Li, S.; Thomas, A.; Kotov, N. A.; Haag, R. Functional Graphene Nanomaterials Based Architectures: Biointeractions, Fabrications, and Emerging Biological Applications. *Chem. Rev.* **2017**, *117*, 1826−1914.
(6) Tan, C.; Cao, X.; Wu, X.-J.; He, Q.; Yang, J.; Zhang, X.; Chen, J.; Zhao, W.; Han, S.; Nam, G.-H.; Sindoro, M.; Zhang, H. Recent Advances in Ultrathin Two-Dimensional Nanomaterials. *Chem. Rev.* **2017**, *117*, 6225−6331.
(7) Boott, C. E.; Nazemi, A.; Manners, I. Synthetic Covalent and Non-Covalent 2D Materials. *Angew. Chem., Int. Ed.* **2015**, *54*, 13876−13894.
(8) Hudson, Z. M.; Boott, C. E.; Robinson, M. E.; Rupar, P. A.; Winnik, M. A.; Manners, I. Tailored hierarchical micelle architectures using living crystallization-driven self-assembly in two dimensions. *Nat. Chem.* **2014**, *6*, 893−898.
(9) Qiu, H.; Gao, Y.; Boott, C. E.; Gould, O. E. C.; Harniman, R. L.; Miles, M. J.; Webb, S. E. D.; Winnik, M. A.; Manners, I. Uniform patchy and hollow rectangular platelet micelles from crystallizable polymer blends. *Science* **2016**, *352*, 697−701.
(10) He, X.; Hsiao, M.-S.; Boott, C. E.; Harniman, R. L.; Nazemi, A.; Li, X.; Winnik, M. A.; Manners, I. Two-dimensional assemblies from crystallizable homopolymers with charged termini. *Nat. Mater.* **2017**, *16*, 481−488.
(11) Arno, M. C.; Inam, M.; Coe, Z.; Cambridge, G.; Macdougall, L. J.; Keogh, R.; Dove, A. P.; O'Reilly, R. K. Precision Epitaxy for Aqueous 1D and 2D Poly(ε-caprolactone) Assemblies. *J. Am. Chem. Soc.* **2017**, *139*, 16980−16985.
(12) Fukui, T.; Kawai, S.; Fujinuma, S.; Matsushita, Y.; Yasuda, T.; Sakurai, T.; Seki, S.; Takeuchi, M.; Sugiyasu, K. Control over differentiation of a metastable supramolecular assembly in one and two dimensions. *Nat. Chem.* **2017**, *9*, 493−499.
(13) Sasaki, N.; Mabesoone, M. F. J.; Kikkawa, J.; Fukui, T.; Shioya, N.; Shimoaka, T.; Hasegawa, T.; Takagi, H.; Haruki, R.; Shimizu, N.; Adachi, S.-I.; Meijer, E. W.; Takeuchi, M.; Sugiyasu, K. Supramolecular double-stranded Archimedean spirals and concentric toroids. *Nat. Commun.* **2020**, *11*, 3578.
(14) Ogi, S.; Sugiyasu, K.; Manna, S.; Samitsu, S.; Takeuchi, M. Living supramolecular polymerization realized through a biomimetic approach. *Nat. Chem.* **2014**, *6*, 188−195.
(15) Kang, J.; Miyajima, D.; Mori, T.; Inoue, Y.; Itoh, Y.; Aida, T. A rational strategy for the realization of chain-growth supramolecular polymerization. *Science* **2015**, *347*, 646−651.
(16) Weyandt, E.; Leanza, L.; Capelli, R.; Pavan, G. M.; Vantomme, G.; Meijer, E. W. Controlling the length of porphyrin supramolecular polymers via coupled equilibria and dilution-induced supramolecular polymerization. *Nat. Commun.* **2022**, *13*, 248.
(17) Wehner, M.; Röhr, M. I. S.; Bühler, M.; Stepanenko, V.; Wagner, W.; Würthner, F. Supramolecular Polymorphism in One-Dimensional Self-Assembly by Kinetic Pathway Control. *J. Am. Chem. Soc.* **2019**, *141*, 6092−6107.
(18) Liu, Y.; Gong, Y.; Guo, Y.; Xiong, W.; Zhang, Y.; Zhao, J.; Che, Y.; Manners, I. Emergent Self-Assembly Pathways to Multidimensional Hierarchical Assemblies using a Hetero-Seeding Approach. *Chem. − Eur. J.* **2019**, *25*, 13484−13490.
(19) Ogi, S.; Matsumoto, K.; Yamaguchi, S. Seeded Polymerization through the Interplay of Folding and Aggregation of an Amino-Acid-based Diamide. *Angew. Chem., Int. Ed.* **2018**, *57*, 2339−2343.
(20) Wan, Q.; To, W.-P.; Yang, C.; Che, C.-M. The Metal−Metal-to-Ligand Charge Transfer Excited State and Supramolecular Polymerization of Luminescent Pincer PdII−Isocyanide Complexes. *Angew. Chem., Int. Ed.* **2018**, *57*, 3089−3093.
(21) Greciano, E. E.; Matarranz, B.; Sánchez, L. Pathway Complexity Versus Hierarchical Self-Assembly in N-Annulated Perylenes: Structural Effects in Seeded Supramolecular Polymerization. *Angew. Chem., Int. Ed.* **2018**, *57*, 4697−4701.
(22) Liu, Y.; Peng, C.; Xiong, W.; Zhang, Y.; Gong, Y.; Che, Y.; Zhao, J. Two-Dimensional Seeded Self-Assembly of a Complex Hierarchical Perylene-Based Heterostructure. *Angew. Chem., Int. Ed.* **2017**, *56*, 11380−11384.
(23) Robinson, M. E.; Nazemi, A.; Lunn, D. J.; Hayward, D. W.; Boott, C. E.; Hsiao, M.-S.; Harniman, R. L.; Davis, S. A.; Whittell, G. R.; Richardson, R. M.; De Cola, L.; Manners, I. Dimensional Control and Morphological Transformations of Supramolecular Polymeric Nanofibers Based on Cofacially-Stacked Planar Amphiphilic Platinum(II) Complexes. *ACS Nano* **2017**, *11*, 9162−9175.
(24) Ma, X.; Zhang, Y.; Zhang, Y.; Liu, Y.; Che, Y.; Zhao, J. Fabrication of Chiral-Selective Nanotubular Heterojunctions through Living Supramolecular Polymerization. *Angew. Chem., Int. Ed.* **2016**, *55*, 9539−9543.
(25) Aliprandi, A.; Mauro, M.; De Cola, L. Controlling and imaging biomimetic self-assembly. *Nat. Chem.* **2016**, *8*, 10−15.
(26) Ogi, S.; Stepanenko, V.; Sugiyasu, K.; Takeuchi, M.; Würthner, F. Mechanism of Self-Assembly Process and Seeded Supramolecular Polymerization of Perylene Bisimide Organogelator. *J. Am. Chem. Soc.* **2015**, *137*, 3300−3307.
(27) Rao, K. V.; Miyajima, D.; Nihonyanagi, A.; Aida, T. Thermally bisignate supramolecular polymerization. *Nat. Chem.* **2017**, *9*, 1133−1139.
(28) Li, Y.; Cai, Z.; Liu, S.; Zhang, H.; Wong, S. T. H.; Lam, J. W. Y.; Kwok, R. T. K.; Qian, J.; Tang, B. Z. Design of AIEgens for near-infrared IIb imaging through structural modulation at molecular and morphological levels. *Nat. Commun.* **2020**, *11*, 1255.
(29) Liu, S.; Zhou, X.; Zhang, H.; Ou, H.; Lam, J. W. Y.; Liu, Y.; Shi, L.; Ding, D.; Tang, B. Z. Molecular Motion in Aggregates: Manipulating TICT for Boosting Photothermal Theranostics. *J. Am. Chem. Soc.* **2019**, *141*, 5359−5368.
(30) Cheng, C.; Gong, Y.; Guo, Y.; Cui, L.; Ji, H.; Yuan, H.; Jiang, L.; Zhao, J.; Che, Y. Long-Range Exciton Migration in Coassemblies: Achieving High Photostability without Disrupting the Electron Donation of Fluorene Oligomers. *Angew. Chem., Int. Ed.* **2021**, *60*, 5827−5832.

https://doi.org/10.1021/jacs.2c07480
J. Am. Chem. Soc. 2022, 144, 15403−15410